

Application of crystal plasticity modeling in equal channel angular extrusion

Sai-yi LI^{1,2}

1. School of Materials Science and Engineering, Central South University, Changsha 410083, China;

2. Key Laboratory of Nonferrous Metal Materials Science and Engineering, Ministry of Education, Central South University, Changsha 410083, China

Received 10 November 2012; accepted 10 December 2012

Abstract: Some applications of crystal plasticity modeling in equal channel angular extrusion (ECAE) of face-centered cubic metals were highlighted. The results show that such simulations can elucidate the dependency of grain refinement efficiency on processing route and the directionality of substructure development, which cannot be explained by theories that consider only the macroscopic deformation behavior. They can also capture satisfactorily the orientation stability and texture evolution under various processing conditions. It is demonstrated that crystal plasticity models are useful tools in exploring the crystallographic nature of grain deformation and associated behavior that are overlooked or sometimes erroneously interpreted by existing phenomenological theories.

Key words: severe plastic deformation; equal channel angular extrusion; texture; crystal plasticity; strain path; grain refinement

1 Introduction

As one of the major severe plastic deformation (SPD) techniques, equal channel angular extrusion (ECAE) has been successfully applied to produce ultrafine-grained bulk metallic materials with an average grain size down to 100 nm [1,2]. Materials processed after ECAE may achieve a high strength at relatively low temperatures and potential superplasticity at high temperatures and high strain rates. During ECAE, a billet is pressed through two channels with equal cross-section, intersecting at an angle Φ (Fig. 1). As the cross-sectional shape of the billet remains nearly the same, the process can be repeated for multiple passes to achieve a significantly high strain level and the accumulated plastic deformation depends mainly on Φ and the number of passes. In multi-pass ECAE, different processing routes can be set up by adjusting the rotation angle (χ , see Fig. 1) of the billet around its longitudinal axis between successive passes. The three basic processing routes that have been widely studied are known to be *A* ($\chi=0^\circ$), *B* (or *B_C*, $\chi=90^\circ$) and *C* ($\chi=180^\circ$) [2]. To date, numerous studies have been carried out to investigate the

microstructure development, texture evolution and mechanical properties in ECAE-processed materials, with emphasis on the effects of various processing parameters, such as the die angle, pass number and processing route [2]. These researches lead to a significant progress in understanding the material behavior during ECAE at different scales.

In addition to the macroscopic deformation behavior, the mesomechanical behavior and the resulting grain refinement and texture evolution are critical aspects in establishing the deformation theory for ECAE. Compared with other deformation processes, such as rolling and conventional extrusion, ECAE is unique in terms of not only the shear-type SPD introduced in each pass but also the unavoidable strain path changes (SPCs) between successive passes. Both SPD and SPC have a significant impact on the material behavior and challenge the current understanding of microstructure and texture development during plastic deformation. Complementary to the detailed observations by various experimental techniques such as transmission electron microscopy (TEM), electron backscatter diffraction (EBSD) and X-ray diffraction (XRD) measurements, crystal plasticity modeling has proven to be useful in studying the material

Foundation item: Projects (50871040, 51271204) supported by the National Natural Science Foundation of China; Project (2012CB619500) supported by the National Basic Research Program of China; Project (NCET-06-0741) supported by the Program for New Century Excellent Talents, China

Corresponding author: Sai-yi LI; Tel: +86-731-88876621; E-mail: saiyi@csu.edu.cn
DOI: 10.1016/S1003-6326(13)62444-9

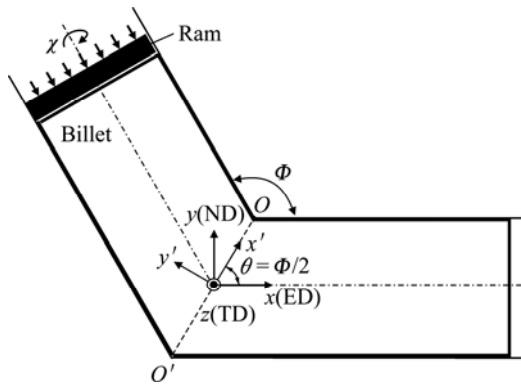


Fig. 1 Schematic diagram of die geometry and billet rotation in ECAE and coordinate systems considered

behavior during plastic deformation. It directly accounts for the crystallographic nature of grains in polycrystalline materials, such as grain orientations, slip or twinning mechanisms, and grain interactions [3–5].

In this work, some typical applications of the crystal plasticity modeling in ECAE of face-centered cubic (FCC) metals are presented. We start with a very brief review of the main features of the macroscopic deformation in Section 1. In Section 2, crystal plasticity models are applied to explaining the dependency of grain refinement efficiency on processing route and the directionality of substructure development. In Section 3, the basic tendencies of texture evolution are reviewed with an emphasis on the heterogeneity of textures and the effects of various processing variables. It is shown that crystal plasticity simulations are very useful in exploring the mesoscopic deformation behavior under SPD and SPCs. They lead to insights into the underlying mechanisms of grain deformation which are overlooked or sometimes erroneously interpreted by existing phenomenological theories.

2 Macroscopic deformation behavior

2.1 Approximation by simple shear

A sound knowledge of the macroscopic deformation behavior in ECAE is a prerequisite in understanding the process–structure–property relationships and in optimization of tool designs and processing variables. To date, many theoretical (analytical or numerical) and experimental studies have been conducted to investigate the macroscopic deformation in ECAE. It is well demonstrated that [1,6] under the ideal conditions the billet deformation during each pass of ECAE can be considered as simple shear on the intersection plane (IP, parallel to OO' in Fig. 1). SEGAL [1] proposed an analytical expression to estimate the shear strain from the die angle Φ . Later, a modified form was proposed by IWAHASHI et al [7] to further incorporate the effect of

the outer corner angle (Ψ). According to their model, the effective strain (ε) per pass can be calculated by

$$\varepsilon = \frac{1}{\sqrt{3}} \left[2 \cot \left(\frac{\Phi}{2} + \frac{\Psi}{2} \right) + \Psi \operatorname{cosec} \left(\frac{\Phi}{2} + \frac{\Psi}{2} \right) \right] \quad (1)$$

Meanwhile, numerical modeling based on the finite element (FE) method has been extensively utilized to evaluate the effect of various influential factors on the deformation behavior, including material constitutive behavior, die geometry, and processing variables (friction, backpressure, temperature, etc.). These investigations, accompanied by experimental verifications, demonstrated that under the realistic conditions the deformation in ECAE is heterogeneous along both the length and the cross-section of the billet, and deviates in various extents from simple shear, although simple shear on the IP plane is still a reasonable approximation of the deformation in the central region of the billet [8,9].

2.2 Strain path changes

While the strain path in each ECAE pass can be idealized to be monotonic or linear with the deformation mode close to simple shear, the ones in multiple passes involve complex changes and are thus nonlinear. In the framework of continuum mechanics, the strain path change (SPC) in a sequential deformation process can be conveniently quantified by considering the directionality of the corresponding strain-rate tensors in each stage [10]. Accordingly, the magnitude of SPC between two successive passes in ECAE is a function of the die angle and billet rotation (or processing route) [11]:

$$\eta = \cos \chi - \frac{1}{2} \sin^2 \Phi (1 + \cos \chi)^2, \quad (2)$$

assuming simple shear in each pass. Since Φ cannot be 0 or 180° in ECAE by definition, the strain path during multi-pass processing cannot be monotonic, regardless of the rotation angle or processing route.

Figure 2 shows the variation of the SPC parameter

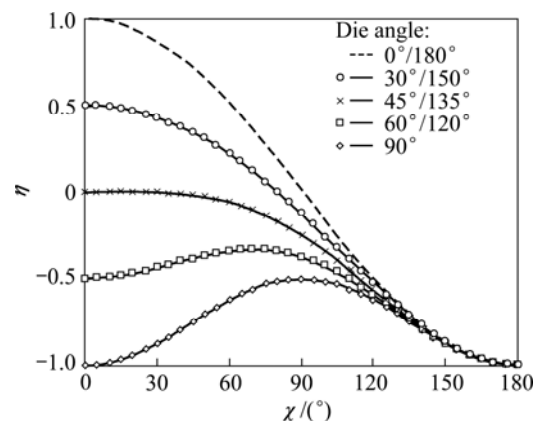


Fig. 2 Variation of SPC parameter with billet rotation in ECAE with different die angles

η with billet rotation for selected Φ values. It is seen that the SPC in route *C* ($\chi=180^\circ$) is always strain reversal ($\eta=-1.0$), but that in routes *A* ($\chi=0^\circ$) and *B* ($\chi=90^\circ$) varies considerably with Φ . For route *A*, the SPC varies from strain reversal for $\Phi=90^\circ$ to a quasi-orthogonal type ($\eta=-0.5$) for $\Phi=120^\circ$. DUPUY and RAUCH [11] showed that the SPC parameter is helpful in understanding the grain refinement process in multi-pass ECAE with different processing routes.

3 Mesomechanical behavior

3.1 Grain refinement under strain path changes

The magnitude of grain refinement in ECAE generally increases with the accumulated plastic deformation, which in turn depends on the die angle and the number of passes. The processing route defined according to the rotation of the billet between successive passes (see Fig. 1) is another important factor that has attracted great attention and also led to significant disputations in both experimental and theoretical studies. For FCC metals, a considerable number of experimental studies have demonstrated that the optimal processing route varies with the die angle. Among the three basic routes, the efficiency of grain refinement is generally found to be the highest with route *B* for $\Phi=90^\circ$ and route *A* for $\Phi=120^\circ$ [12,13]. Several theories have been proposed to interpret such dependencies by considering various characteristics of macroscopic deformation, such as the intersection of shear planes [14], redundant strain [13] or SPC [11]. However, none of these theories could consistently explain the relative efficiencies of grain refinement associated with different Φ values. The neglect of the crystallographic nature of plastic deformation is a major deficiency in these theories.

Crystal plasticity modeling of the slip activities accounting for the deformation mechanisms under given macroscopic deformation conditions is an efficient way to overcome this deficiency. Preliminary simulations have provided insights into the grain refinement under SPCs [15,16]. For FCC metals, for example, simulations have been performed for multi-pass ECAE via the three basic routes with $\Phi=90^\circ$ and 120° , respectively, using a visco-plasticity self-consistent (VPSC) model. Unlike the classical full-constraint Taylor model, in which the local strain rates in the grains are enforced to be equal to the macroscopic strain rate applied to a polycrystal, the VPSC model allows each grain to deform differently, depending on its directional properties and the strength of the interaction with its surroundings [17]. The material was assumed to have an initial random orientation distribution. During each ECAE pass the macroscopic deformation was assumed to be simple shear on the IP plane. The plastic deformation was accommodated by

dislocation glide on the $\{111\}\langle 110 \rangle$ slip systems with equal critical resolved shear stresses and no hardening for all slip systems. Statistic data in terms of the average number of active slip systems per grain were then computed for each increment, i , by comparing the simulation results at that increment and those of the previous one, $i-1$. This set of data includes: 1) N_{all} for all active systems in increment i ; 2) N_{new} for systems newly activated in increment i ; and 3) N_{rev} for systems that are active in both increments while the slip direction is reversed.

Figure 3 shows the average number of active slip systems stated above as a function of pass number for the three basic routes with $\Phi=90^\circ$ and route *A* with $\Phi=120^\circ$. It can be seen that the effects of the processing route and Φ on the N_{new} and N_{rev} values are more significant than those on N_{all} , especially at the transitions between successive passes. For route *A* (Fig. 3(a)) or *C* (Fig. 3(c)) with $\Phi=90^\circ$, the N_{rev} values at these transitions are much higher than the N_{new} values. This means that, upon reloading in a subsequent pass, the active slip systems for the majority of the grains are dominated by the ones that have reversed the slip directions, while the contributions of the newly activated systems are small. For the same Φ in route *B* (Fig. 3(b)), the N_{new} values at the transitions become higher than those of N_{rev} , indicating a larger contribution from the newly activated systems than the reversed ones. When Φ is changed to be 120° , the characteristic slip activities at the pass-to-pass transitions change little for routes *B* and *C*. For route *A* (Fig. 3(d)), however, the N_{new} values at the transitions become higher than those of N_{rev} , in great contrast to those of $\Phi=90^\circ$ (Fig. 3(a)). Similar tendencies are found in crystal plasticity simulations using the Taylor model which neglects the interactions between grains [15].

Since the activation of new slip systems is known to facilitate the accumulation of dislocations and hence promote the grain subdivision during plastic deformation, the relative efficiencies of grain refinement in the different cases can be compared according to the contribution of newly activated slip systems at the pass-to-pass transitions in terms of the normalized average number of newly activated slip systems [15,16]:

$$\rho_{\text{new}} = \frac{1}{k-1} \sum_{n=2}^k \frac{N_{\text{new}}^n}{N_{\text{all}}^n} \times 100\% \quad (3)$$

where N_{all}^n and N_{new}^n denote the average numbers of all active slip systems and newly activated slip systems, respectively, for the first increment in the n -th pass, and k stands for the total number of passes (here, $k=8$). As shown in Fig. 4, the ρ_{new} values thus calculated change considerably with the processing route and die angle. The order of grain refinement efficiency for the

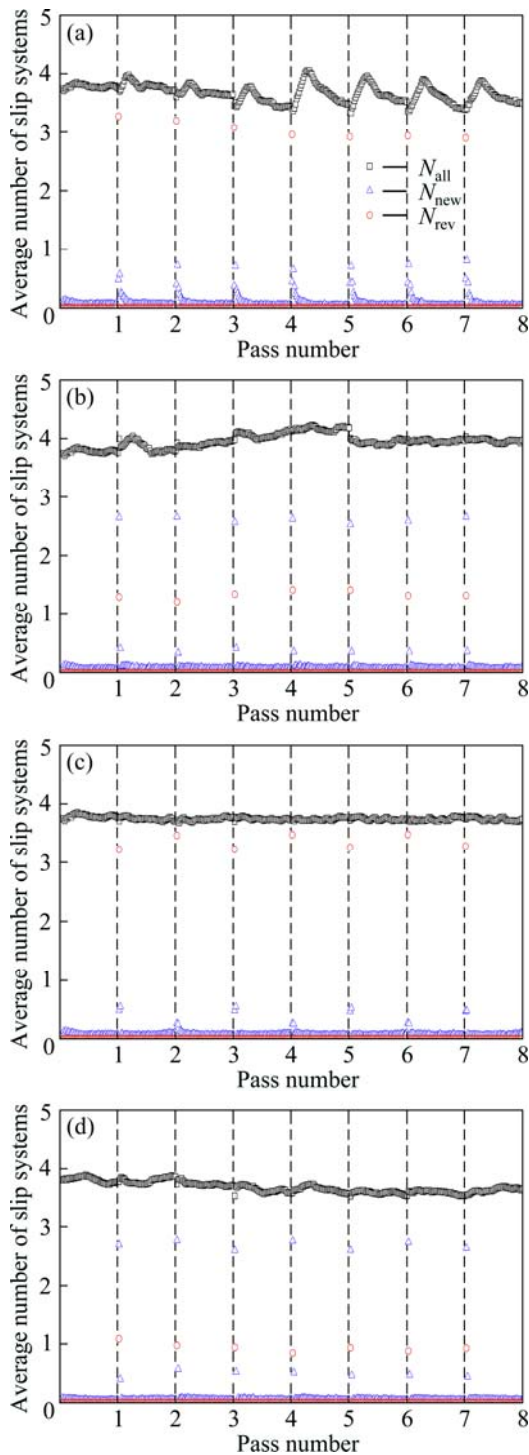


Fig. 3 Variation of average number of various slip systems in ECAE via routes A (a), B (b) and C (c) with $\Phi=90^\circ$ and route A with $\Phi=120^\circ$ (d) [16]

three routes is then predicted to be $B > A \geq C$ for $\Phi=90^\circ$, and $A \geq B > C$ for $\Phi=120^\circ$. These results agree with the relative efficiencies of grain refinement observed in Al and Al alloys [12,13], except that for $\Phi=90^\circ$ the experimental observations suggest a slightly higher efficiency for route C than route A [12], whereas the opposite is anticipated from the simulations.

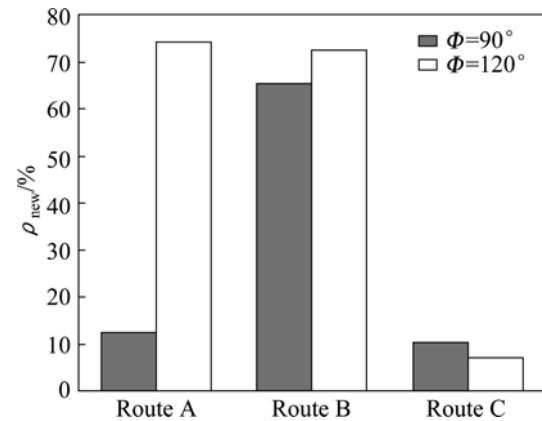


Fig. 4 Normalized average number of newly activated slip systems (ρ_{new}) at pass-to-pass transitions in ECAE with different die angles and processing routes [16]

It is worthwhile to note that the SPC parameter defined based on the macroscopic deformation has been applied, with some success, to explain the dependency of grain refinement on the processing route for $\Phi=90^\circ$, assuming that an orthogonal-type SPC is beneficial for rapid grain refinement [11]. However, it is evident from the crystal plasticity simulations that the same macroscopic SPC does not necessarily lead to the same mesoscopic deformation at the grain level, even in the sense of statistical slip activities. Proper consideration of the mesomechanical behavior is indispensable in understanding the grain refinement process under SPCs.

3.2 Directionality of slip traces and substructures

The microstructure development in ECAE generally fits within the framework of grain subdivision by dislocation boundaries, which has been well established for FCC metals deformed to large strains [5]. Similar to those in other deformation processes, banded structures consisting of elongated subgrains and aligning along the primary slip plane traces are often observed in ECAE-processed metals [12,14,18–22]. As an effort to explain such observations, the so-called shearing patterns have been derived by assuming simple shear on the IP plane of the two channels and then considering the intersections of this shear plane with the three orthogonal inspection planes of the billet [12,14]. These shearing patterns were then practically taken as slip patterns and it was concluded that the banded structures are aligned along directions parallel to the traces of these patterns [14]. A key question is that whether the shearing patterns can be simply taken as the slip patterns.

The slip activities during plastic deformation of polycrystals depend not only on the macroscopic deformation, but also on the grain orientations and grain intersections. To investigate statistically the slip traces developed in ECAE and their relevance to the

directionality of banded structures in comparison with the shearing patterns, a statistical analysis of the slip traces was performed [23] based on the slip activities from VPSC crystal plasticity simulations assuming idealized simple shear on the intersection plane under similar conditions as those considered in Section 3.1. As illustrated in Fig. 5, the slip traces of an active slip system are the intersections of that slip plane with the three inspection planes perpendicular to the x , y , and z axes, respectively. Their directionality can be measured by three angles: α_x defines the inclination angle to the y -axis on the x -plane, α_y angle to z -axis on y -plane, and α_z angle to x -axis on z -plane. Though multiple slip systems are generally activated in each grain, only the one generating the maximum shear rate was considered in the statistics as this slip system is expected to contribute the most to the substructure development.

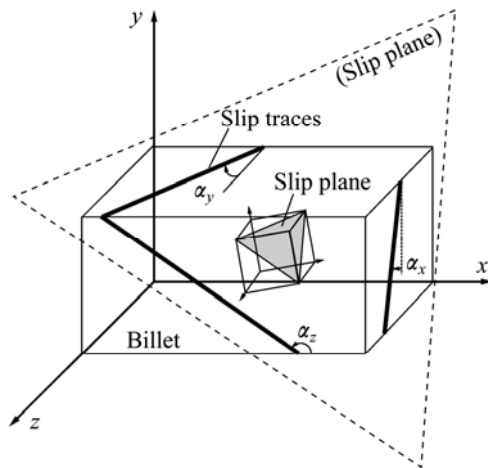


Fig. 5 Schematic illustration of slip traces generated by intersections of a slip plane in a crystal with the macroscopic sectioning planes in ECAE-processed billet lying in the outlet channel [23]

Figure 6 shows the distributions of slip trace angles simulated for one pass of ECAE with $\Phi=90^\circ$ and $\Phi=120^\circ$. It is seen that the slip trace angles are widely spread in the theoretical angular range due to the orientation-dependency of grain deformation. Interestingly, preferred directions are evident on each of the inspection planes. The α_x and α_y angles show moderate preferences near 90° and 0° or 180° , respectively, indicating that the slip traces are aligned preferentially along directions parallel to the z -axis on both the x - and y -planes. The distribution of α_z shows two peaks at about $\Phi/2$ and $\Phi/2+90^\circ$, and indicates that the slip traces on the z -plane are preferentially parallel and perpendicular, respectively, to the macroscopic shear plane (MSP) or IP. These directionalities of slip traces agree well with those of banded structures found in various polycrystal experiments [12,19,20].

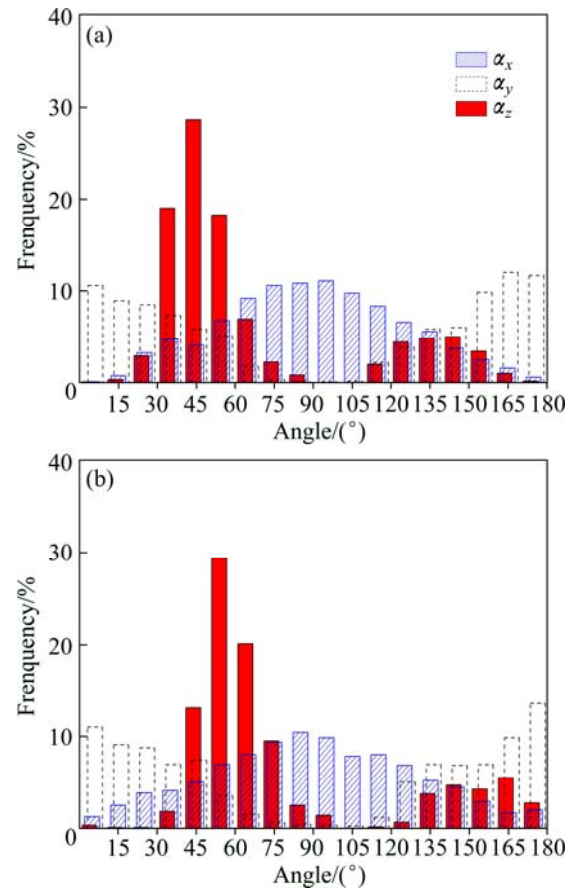


Fig. 6 Alignment of slip traces simulated after one pass of ECAE with $\Phi=90^\circ$ (a) and $\Phi=120^\circ$ (b) [23]

This crystal-plasticity-based analysis substantiates that the directions of banded structures are closely linked to the alignment of slip traces, which depends on the deformation behavior at both the macro- and mesoscopic scales. It is noted that the directions of the imaginary slip traces derived from the shearing pattern [12,14] would correspond to a single set of angles with $\alpha_x=90^\circ$, $\alpha_y=0^\circ$ (or 180°) and $\alpha_z=\Phi/2$, and thus coincide with the primary preferred directions of the predicted slip traces. The other details of the slip trace alignments, such as their wide spreading on each of the inspection planes and the secondary preferred direction on the z -plane near $\alpha_z=\Phi/2+90^\circ$, could not be deduced from the shearing patterns at all. Overall, it is misleading to apply the shearing patterns to interpret microstructure observations without paying sufficient attention to their fundamental differences with the slip patterns.

4 Texture evolution

The SPD involved in the ECAE process results in significant changes of crystallographic texture in the billet. The evolution of texture in turn can potentially modify the anisotropy in the physical and mechanical

properties of the processed material. To date, both experimental and theoretical investigations on the texture evolution in ECAE have been carried out for a large number of materials, as a function of various processing variables, such as pass number, die angle and processing route. In particular, crystal plasticity simulations contribute significantly to the understanding of the basic tendencies of texture evolution in FCC metals. In these simulations, two types of approaches are often considered. One is a combination of polycrystal models (e.g. Taylor and VPSC) with an idealized simple-shear or FE-prediction description of the macroscopic deformation [24,25], and the other is the direct application of the crystal plasticity finite element (CPFE) models [26–28]. The latter approach is in general more accurate in reflecting the grain interactions than the former approach, but is very time-consuming and difficult to apply realistic boundary conditions. Here, several applications of the former approach are presented, with an emphasis on the orientation stability and heterogeneity in single pass and the major features of texture evolution in multiple passes.

4.1 Ideal orientations

Ideal orientations are important information in analyzing the characteristics of textures or the main texture components during plastic deformation. For ECAE, the ideal orientations were first identified in investigations of texture evolutions in polycrystalline materials [24,25,29], and latter confirmed with the help of orientation stability analysis [30]. It was found that [29] the main texture components after a single-pass ECAE are distributed along orientation fibers featured by a crystallographic $\{111\}$ -plane CCW-rotated for θ ($\theta = \Phi/2$, see Fig. 1) around TD from the ND-plane, or a $\langle 110 \rangle$ -direction CCW-rotated by θ around TD from the ED. The corresponding ideal orientations identified from experimental studies, as listed in Table 1 and illustrated

in the key (111) pole figure of Fig. 7 for the case of $\Phi = 90^\circ$ [29,31], are consistent with those derived for negative simple shear by a rotation about the flow plane normal. Common to both ECAE and simple shear, the ideal orientations are distributed along fibers in the orientation space, with the slip plane and slip direction parallel to the MSP and macroscopic shear direction, respectively.

Since an experimental or simulated texture in a polycrystalline material is obtained from an average of numerous final grain orientations, these studies do not directly reveal the flow behavior and orientation stability of individual grains. A direct assessment of the orientation stability was carried out based on the rotation velocity vector $\dot{\mathbf{R}} = (\dot{\varphi}_1, \dot{\phi}, \dot{\varphi}_2)$ derived from single crystal plasticity calculations of single crystal in the orientation space [30]. In this analysis, an orientation $\mathbf{g} = (\varphi_1, \phi, \varphi_2)$ in Bunge's notation is considered to be a stable end orientation during plastic deformation when the three components of $\dot{\mathbf{R}}$ are equal to zero and their first-order partial derivatives are negative, i.e.,

$$\dot{\varphi}_1 = 0, \quad \dot{\phi} = 0, \quad \dot{\varphi}_2 = 0 \quad (4)$$

$$\frac{\partial \dot{\varphi}_1}{\partial \varphi_1} < 0, \quad \frac{\partial \dot{\phi}}{\partial \phi} < 0, \quad \frac{\partial \dot{\varphi}_2}{\partial \varphi_2} < 0 \quad (5)$$

It is shown that the experimentally determined ideal orientations from polycrystalline FCC metals as shown in Table 1 are meta-stable orientations and there are no real stable orientations in ECAE deformation [30].

4.2 General observations in multiple passes

In multi-pass ECAE, the texture evolution in a succeeding pass can be affected by the texture developed during the preceding pass, and such entry texture effects depend on the processing route and die geometry. The mesomechanical behavior and the corresponding texture development are also complicated due to the characteristic

Table 1 Euler angles and Miller indices of main ideal orientations in ECAE of FCC crystals with $\Phi = 90^\circ$ [31]

Notation	Euler angles/(°)			Miller indices			Equivalent representation with TD-rotation by $\theta(45^\circ)$
	φ_1	ϕ	φ_2	ND	ED	TD	
$A_{1\theta}^*$	80.26/260.26	45	0	$[\bar{1} \bar{1} \bar{8}]$	$[44 \bar{1}]$	$[\bar{1} 10]$	$(111)[\bar{1} \bar{1} 2]_\theta$
	170.26/350.26	90	45				
$A_{2\theta}^*$	9.74/189.74	45	0	$[\bar{4} 4 1]$	$[118]$	$[1 \bar{1} 0]$	$(111)[1 \bar{1} 2]_\theta$
	99.74/279.74	90	45				
A_θ	45	35.26	45	$[1 11 \bar{5}]$	$[914]$	$[\bar{1} 12]$	$(\bar{1} \bar{1} 1)[110]_\theta$
\bar{A}_θ	225	35.26	45	$[\bar{1} \bar{1} 1 5]$	$[\bar{9} \bar{1} 4]$	$[\bar{1} 12]$	$(\bar{1} \bar{1} \bar{1})[\bar{1} \bar{1} 0]_\theta$
B_θ	45/165/285	54.74	45	$[7 26 \bar{1} 9]$	$[15 4 11]$	$[\bar{1} 11]$	$(\bar{1} \bar{1} 2)[110]_\theta$
\bar{B}_θ	105/225/345	54.74	45	$[\bar{7} \bar{2} 6 19]$	$[\bar{1} 5 \bar{4} 11]$	$[\bar{1} 11]$	$(\bar{1} \bar{1} 2)[\bar{1} \bar{1} 0]_\theta$
C_θ	135/315	45	0	$[22\bar{3}]$	$[334]$	$[\bar{1} 10]$	$\{001\}\langle 110 \rangle_\theta$
	45/225	90	45				

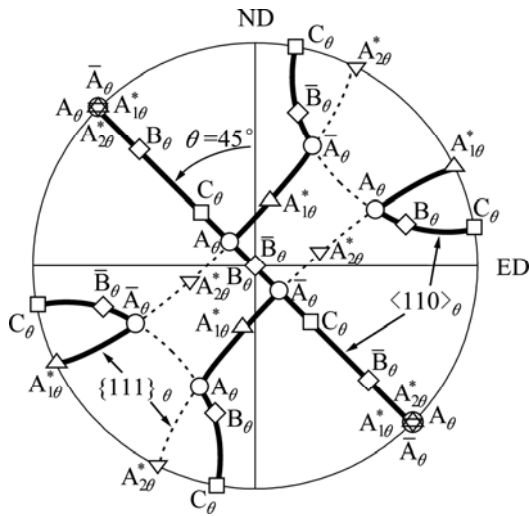


Fig. 7 (111) key pole figure showing ideal orientations in ECAE deformation with $\phi=90^\circ$ [31]

SPCs associated with different processing routes and die geometries.

Figure 8 shows the bulk textures measured by neutron diffraction for pure Cu samples processed after different number of passes via routes *A* and *B*, in comparison with those obtained from VPSC simulations using the FE-predicted deformation history at the center region of the billets [31,32]. These results reveal that the texture development in multi-pass ECAE varies with processing variables, showing characteristic texture features for different processing routes. It is also clear that the ECAE textures always depict orientation concentrations along orientation fibers identified for single pass deformation, though the main texture components vary both in positions (along the fibers) and in intensity. The crystal plasticity predictions can satisfactorily capture the main texture features in the experimental observations. This indicates that, despite the significant changes of entry textures and strain path

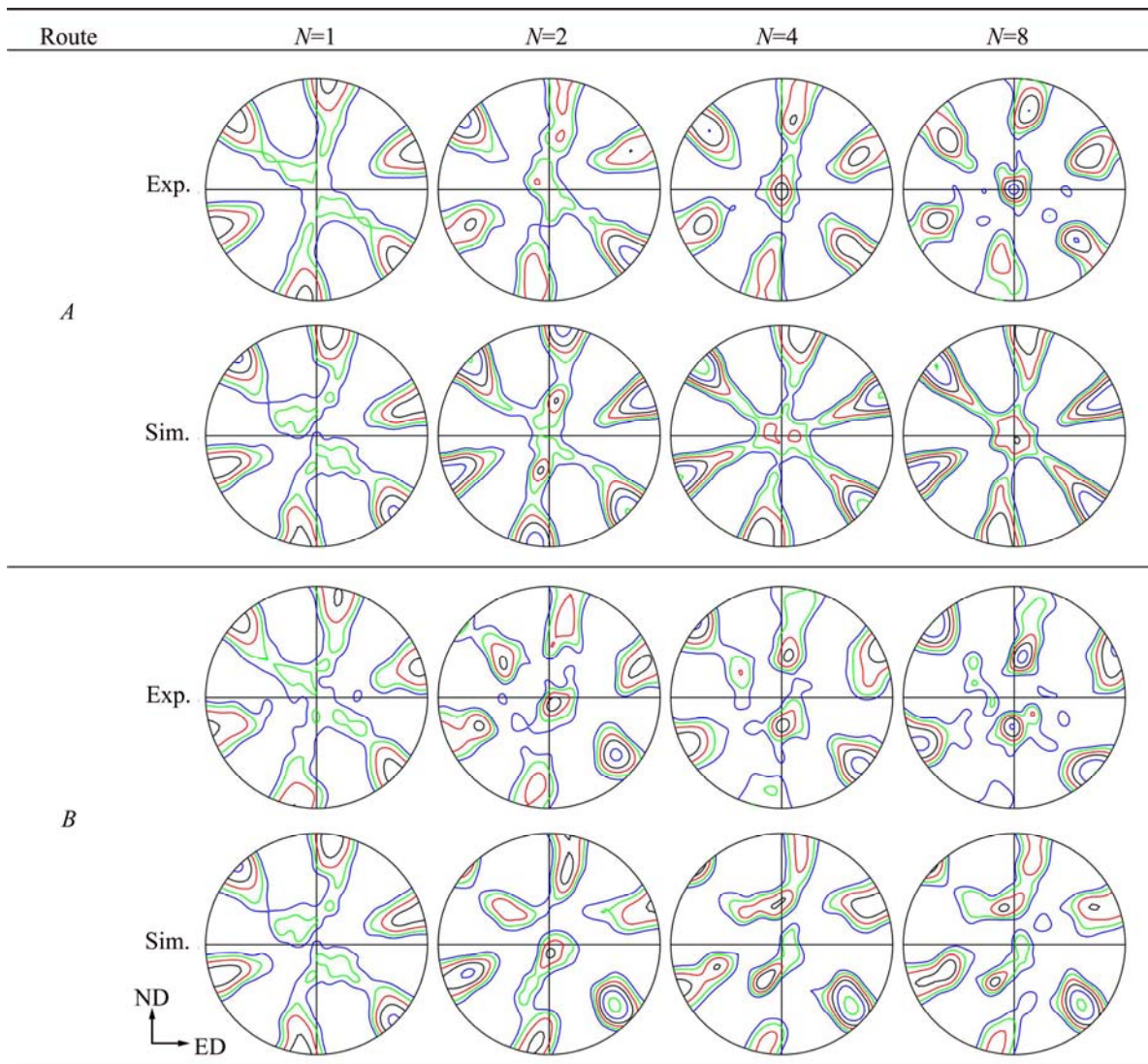


Fig. 8 (111) pole figures of experimental and simulated textures in Cu billets after various passes of ECAE via routes *A* and *B* (Contours: 1/1.4/2.8/4/5.6/8/11/16/22) [31,32]

in multiple passes, the deformation in each pass is large enough to re-orient grains to the ideal fibers such that shear-type textures can be partially re-established at least.

It is interesting to note that from a theoretical point of view, the texture development in route *C* is considered to be the most interesting among all the various processing route studies. For route *C*, it is generally found that the first pass texture is retained in subsequent passes, apart from slight variations in the strengths of the main texture components [32,33]. In particular, the shear textures retained after even-numbered passes have attracted great interest in crystal plasticity modeling. It is recognized that in this case, it is necessary to account for the deformation heterogeneity at the macroscopic level, as well as grain refinement and latent hardening at the single crystal level in order to obtain accurate predictions of the deformation textures [28,32–36]. In this sense, ECAE is a unique process in testing and advancing the crystal plasticity models.

4.3 Heterogeneity

In modeling texture evolution, idealized simple shear is often assumed but nonetheless succeeds in predicting the main features in the experimental textures [24,25,29]. The quality of texture predictions can be further improved by using more realistic deformation histories, which can be provided by experimental grids, FE calculations, or flow models. As noted in Section 2, FE simulations with supporting experimental evidence have demonstrated that the actual deformation in the billet deviates from idealized simple shear and, most importantly, the distribution of deformation in the billet is not uniform. Therefore, the heterogeneity in the resulting textures is another important subject in the application of crystal plasticity simulations to ECAE.

Figure 9 shows the actual shape of a half-way extruded pure Cu billet and the corresponding FE prediction. It is seen that the deformation is non-uniform both through the billet thickness (i.e., along ND) and along the billet length (i.e., along ED). The accumulated strain in the bottom region is apparently less uniform and smaller than those in the top to middle regions. The length of the steady-state region with uniform deformation along the billet length is only about two times of the billet cross-section size.

Figure 10 shows the grain structures and microtextures measured by EBSD at three thickness locations (defined by *s*) [25] in the steady-state region for the same billet shown in Fig. 9. It is evident that both the microstructures and the textures vary with *s*, showing well-developed shear-type structures and textures in the top to middle regions (*s*=0.1–0.5), but a less-deformed structure with a weaker shear-type texture in the bottom

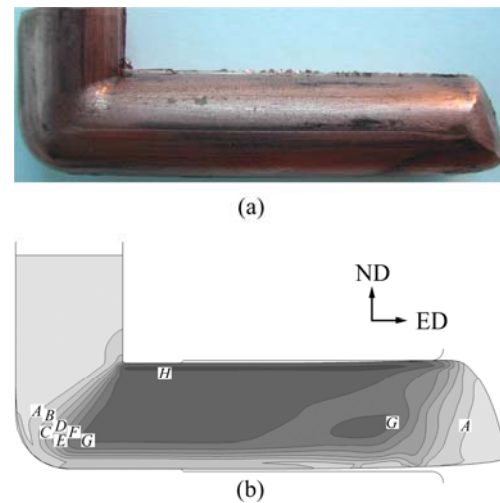


Fig. 9 Photo taken on Cu billet partly pressed through ECAE die (a) and corresponding equivalent plastic strain distribution obtained by FE simulation (b) (The strain levels vary from *A* for 0.15 to *H* for 1.2 at an interval of 0.15 between adjacent characters) [25]

region (*s*=0.9), which are consistent with the deformation heterogeneity. The texture heterogeneities are satisfactorily reproduced by the simulations using a VPSC model with the FE-predicted deformation histories. Although the deformation and texture heterogeneity are significant in a single pass of ECAE, they are expected to decrease with an increase of the number of passes. However, this has been demonstrated for only a very few cases [25,34,37], and a systematic investigation is still lacking.

5 Summary

ECAE is a unique deformation process featuring both SPD by approximate simple shear in each pass and SPCs in multiple passes. Both SPD and SPC have a significant impact on the material behavior and challenge the current understanding of microstructure and texture development during plastic deformation. Complementary to the detailed observations by various experimental techniques, crystal plasticity modeling has proven to be useful in studying the material behavior during plastic deformation as it directly accounts for the crystallographic nature of grains in polycrystalline materials.

In this concise review, some applications of the crystal plasticity modeling in ECAE of FCC metals are highlighted. It is shown that such simulations can elucidate the dependency of grain refinement efficiency on processing route and the directionality of substructure development, which cannot be explained by theories that consider only the macroscopic deformation behavior.

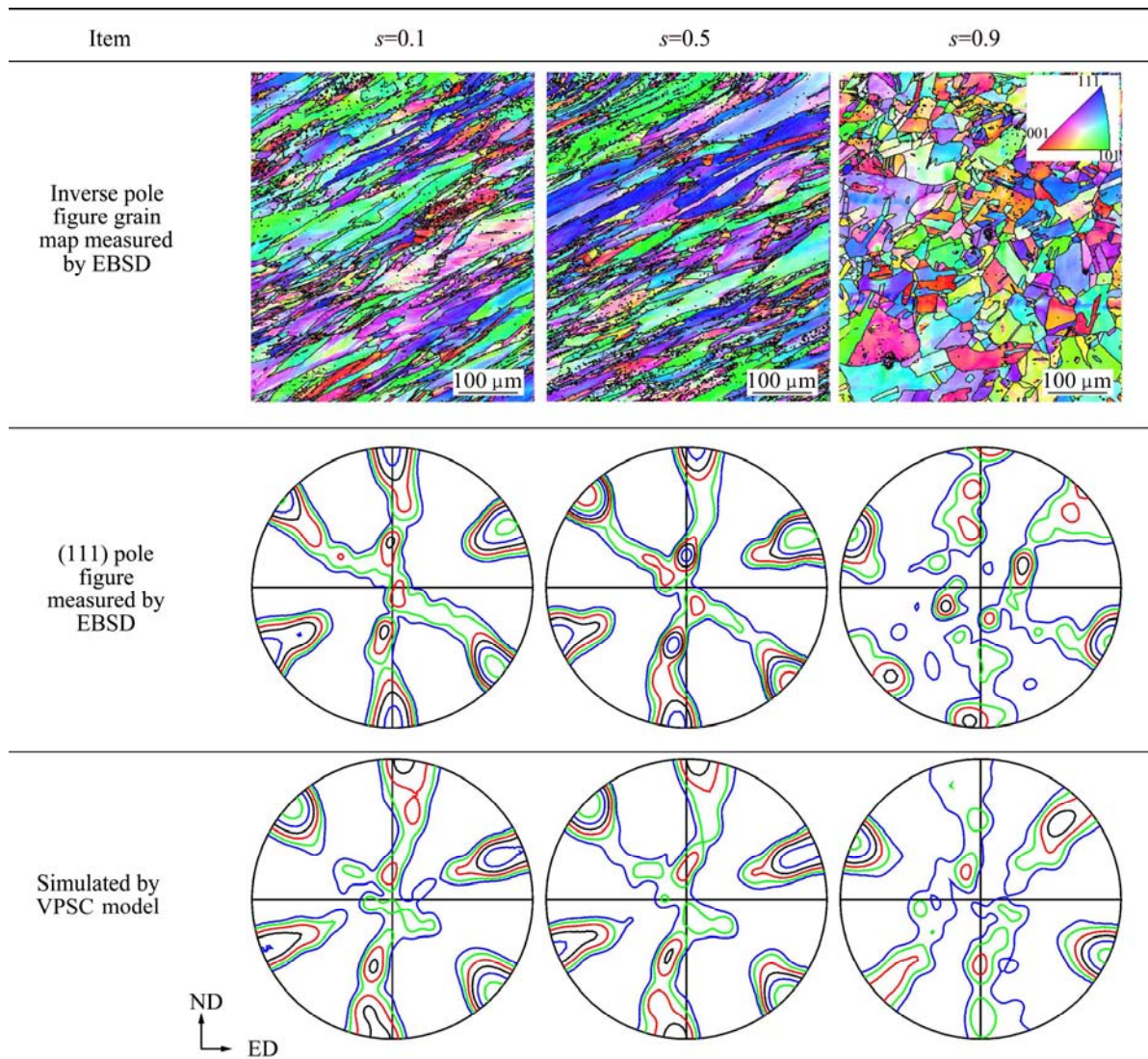


Fig. 10 Variation of microstructures and textures with thickness positions in steady-state region of Cu billet processed after one ECAE pass (Contours: 1/1.4/2/2.8/4/5.6/8/11/16/22) [25]

They can also capture satisfactorily the orientation stability and texture evolution under various processing conditions. Overall, crystal plasticity simulations are very useful in exploring the mesoscopic deformation behavior under SPD and SPCs, and can lead to insights into the underlying mechanisms of grain deformation which are sometimes erroneously interpreted by existing phenomenological theories. The complexity of ECAE deformation also points out directions in future development of crystal plasticity theories and models to improve the modeling of deformation heterogeneity, grain subdivision and latent hardening in a polycrystalline material.

References

- [1] SEGAL V M. Materials processing by simple shear [J]. Mater Sci Eng A, 1995, 197: 157–164.
- [2] VALIEV R Z, LANGDON T G. Principles of equal-channel angular pressing as a processing tool for grain refinement [J]. Prog Mater Sci, 2006, 51: 881–981.
- [3] KOCKS U F, TOME C N, WENK H R. Texture and anisotropy-preferred orientations in polycrystals and their effect on materials properties [M]. Cambridge: Cambridge University Press, 2000.
- [4] ROTERS F, EISENLOHR P, HANTCHERLI L, TJAHLANTO D D, BIELER T R, RAABE D. Overview of constitutive laws, kinematics, homogenization and multiscale methods in crystal plasticity finite-element modeling: Theory, experiments, applications [J]. Acta Mater, 2010, 58: 1152–1211.
- [5] WINTHER G. Slip patterns and preferred dislocation boundary planes [J]. Acta Mater, 2003, 51: 417–429.
- [6] LEE D N. An upper-bound solution of channel angular deformation [J]. Scripta Mater, 2000, 43: 115–118.
- [7] IWAHASHI Y, WANG J, HORITA Z, NEMOTO M, LANGDON T G. Principle of equal-channel angular pressing for the processing of ultra-fine grained materials [J]. Scripta Mater, 1996, 35: 143–146.
- [8] KIM H S, SEO M H, HONG S I. On the die corner gap formation in equal channel angular pressing [J]. Mater Sci Eng A, 2000, 291: 86–90.
- [9] LI S, BOURKE M A M, BEYERLEIN I J, ALEXANDER D J,

- CLAUSEN B. Finite element modeling of the plastic deformation zone and working load in equal channel angular extrusion [J]. *Mater Sci Eng A*, 2004, 382: 217–236.
- [10] SCHMITT J H, AERNOUDT E, BAUDELET B. Yield loci for polycrystalline metals without texture [J]. *Mater Sci Eng*, 1985, 75: 13–20.
- [11] DUPUY L, RAUCH E F. Deformation paths related to equal channel angular extrusion [J]. *Mater Sci Eng A*, 2002, 337: 241–247.
- [12] IWAHASHI Y, HORITA Z, NEMOTO M, LANGDON T G. The process of grain refinement in equal-channel angular pressing [J]. *Acta Mater*, 1998, 46: 3317–3331.
- [13] GHOLINIA A, PRANGNELL P B, MARKUSHEV M V. The effect of strain path on the development of deformation structures in severely deformed aluminium alloys processed by ECAE [J]. *Acta Mater*, 2000, 48: 1115–1130.
- [14] FURUKAWA M, HORITA Z, LANGDON T G. Factors influencing the shearing patterns in equal-channel angular pressing [J]. *Mater Sci Eng A*, 2002, 332: 97–109.
- [15] LI S. A crystal plasticity-based explanation for the dependencies of grain refinement on processing route and die angle in equal channel angular extrusion [J]. *Scripta Mater*, 2009, 60: 706–709.
- [16] LI S. Grain refinement efficiency in equal channel angular extrusion of fcc metals inferred from crystal plasticity simulations of slip activities [J]. *Mater Sci Forum*, 2010, 638–642: 1971–1976.
- [17] TOMÉ C N, LEBENSOHN R A, NECKER C T. Mechanical anisotropy and grain interaction in recrystallized aluminum [J]. *Metall Mater Trans A*, 2002, 33: 2635–2648.
- [18] DALLA TORRE F, LAPOVOK R, SANDLIN J, THOMSON P F, DAVIES C H J, PERELOMA E V. Microstructures and properties of copper processed by equal channel angular extrusion for 1–16 passes [J]. *Acta Mater*, 2004, 52: 4819–4832.
- [19] WU P C, CHANG C P, KAO P W. The distribution of dislocation walls in the early processing stage of equal channel angular extrusion [J]. *Mater Sci Eng A*, 2004, 374: 196–203.
- [20] XUE Q, BEYERLEIN I J, ALEXANDER D J, GREY G T. Mechanisms for initial grain refinement in OFHC copper during equal channel angular pressing [J]. *Acta Mater*, 2007, 55: 655–668.
- [21] MIYAMOTO H, FUSHIMI J, MIMAKI T, VINOGRADOV A, HASHIMOTO S. Dislocation structures and crystal orientations of copper single crystals deformed by equal-channel angular pressing [J]. *Mater Sci Eng A*, 2005, 405: 221–232.
- [22] FUKUDA Y, OH-ISHI K, FURUKAWA M, HORITA Z, LANGDON T G. Influence of crystal orientation on the processing of copper single crystals by ECAP [J]. *J Mater Sci*, 2007, 42: 1501–1511.
- [23] LI S. Directionality of slip traces and banded structures in fcc materials processed by equal-channel angular extrusion [J]. *Scripta Mater*, 2012, 67: 348–351.
- [24] TÓTH L S, MASSION R A, GERMAIN L, BAIK S C, SUWAS S. Analysis of texture evolution in equal channel angular extrusion of copper using a new flow field [J]. *Acta Mater*, 2004, 52: 1885–1898.
- [25] LI S, BEYERLEIN I J, NECKER C T, ALEXANDER D J, BOURKE M. Heterogeneity of deformation texture in equal channel angular extrusion of copper [J]. *Acta Mater*, 2004, 52: 4859–4875.
- [26] KALIDINDI S R, DONOHUE B R, LI S. Modeling texture evolution in equal channel angular extrusion using crystal plasticity finite element models [J]. *Int J Plasticity*, 2009, 25: 768–779.
- [27] LU C, DENG G Y, TIEU A K, SUA S H, ZHU H T, LIU X H. Crystal plasticity modeling of texture evolution and heterogeneity in equal channel angular pressing of aluminum single crystal [J]. *Acta Mater*, 2011, 59: 3581–3592.
- [28] WU P D, HUANG Y, LLOYD D J. Studying grain fragmentation in ECAE by simulating simple shear [J]. *Scripta Mater*, 2006, 54: 2107–2112.
- [29] LI S, BEYERLEIN I J, BOURKE M A M. Texture formation during ECAE of fcc and bcc materials: Comparison with simple shear [J]. *Mater Sci Eng A*, 2005, 394: 66–77.
- [30] LI S. Orientation stability in equal channel angular extrusion. (Part I): Face-centered cubic and body-centered cubic materials [J]. *Acta Mater*, 2008, 56: 1018–1030.
- [31] LI S, BEYERLEIN I J, ALEXANDER D J. Characterization of deformation textures in pure copper processed by equal channel angular extrusion via route A [J]. *Mater Sci Eng A*, 2006, 431: 339–345.
- [32] LI S, BEYERLEIN I J, ALEXANDER D J, VOGEL S C. Texture evolution during multi-pass equal channel angular extrusion of copper: Neutron diffraction characterization and polycrystal modelling [J]. *Acta Mater*, 2005, 53: 2111–2125.
- [33] SUWAS S, ARRUFFAT MASSION R, TÓTH L S, FUNDENBERGER J J, BEAUSIR B. Evolution of texture during equal channel angular extrusion of commercially pure aluminum: Experiments and simulations [J]. *Mater Sci Eng A*, 2009, 520: 134–146.
- [34] LI S, BEYERLEIN I J, NECKER C T. On the development of microstructure and texture heterogeneity for ECAE via route C [J]. *Acta Mater*, 2006, 54: 1397–1408.
- [35] GU C F, TÓTH L S. The origin of strain reversal texture in equal channel angular pressing [J]. *Acta Mater*, 2011, 59: 5749–5757.
- [36] MANESH S, BEYERLEIN I J, TOMÉ C N. Loading- and substructure-induced irreversibility in texture during route C equal channel angular extrusion [J]. *Scripta Mater*, 2005, 53: 965–969.
- [37] SKROTZKI W, SCHEERBAUM N, OERTEL C G, ARRUFFAT MASSION R, SUWAS S, TÓTH L S. Microstructure and texture gradient in copper deformed by equal channel angular pressing [J]. *Acta Mater*, 2007, 55: 2013–2024.

晶体塑性模拟在等通道转角挤压中的应用

李赛毅^{1,2}

1. 中南大学 材料科学与工程学院, 长沙 410083;

2. 中南大学 有色金属材料科学与工程教育部重点实验室, 长沙 410083

摘要: 概述了晶体塑性模拟在面心立方金属等通道转角挤压中的典型应用。结果表明, 这些模拟能够较好地解释仅基于宏观变形行为所不能解释的晶粒细化效率的路径相关性和亚结构方向性问题, 能够满意地预测不同加工条件下材料的晶粒取向稳定性和织构演变。应用表明, 晶体塑性模拟是探索晶粒变形的晶体学特性以及相关行为的有效手段, 而这些特性常常被现有宏观理论所忽略或错误地解释。

关键词: 剧烈塑性变形; 等通道转角挤压; 织构; 晶体塑性; 应变路径; 晶粒细化

(Edited by Xiang-qun LI)